

1 Article

2 

# Using Psychophysiological Sensors to Assess Mental 3 Workload in Web Browsing

4 Angel Jimenez-Molina<sup>1,\*</sup>, Cristian Retamal<sup>2</sup> and Hernan Lira<sup>3</sup>5 <sup>1</sup> University of Chile, Faculty of Physical and Mathematical Sciences, Department of Industrial Engineering;  
6 ajimenez@dii.uchile.cl7 <sup>2</sup> University of Chile, Faculty of Physical and Mathematical Sciences, Department of Electrical Engineering;  
8 cristian.retamal@ug.uchile.cl9 <sup>3</sup> University of Chile, Faculty of Physical and Mathematical Sciences, Department of Industrial Engineering;  
10 hlira@ing.uchile.cl

11 \* Correspondence: ajimenez@dii.uchile.cl; Tel.: +56-2-2978-4056

12 **Abstract:** The mental workload induced by a Web page is essential for improving the user's  
13 browsing experience. However, continuously assessing the mental workload during a browsing  
14 task is challenging. In order to face this issue, this paper leverages the correlation between stimuli  
15 and physiological responses, which are measured with high-frequency, non-invasive  
16 psychophysiological sensors during very short span windows. An experiment was conducted to  
17 identify levels of mental workload through the analysis of pupil dilation measured by an  
18 eye-tracking sensor. In addition, a method was developed to classify real-time mental workload by  
19 appropriately combining different signals (electrodermal activity (EDA), electrocardiogram,  
20 photoplethysmography (PPG), electroencephalogram (EEG), temperature and eye gaze) obtained  
21 with non-invasive psychophysiological sensors. The results show that the Web browsing task  
22 involves on average four levels of mental workload. Also, by combining EEG with the PPG and  
23 EDA, the accuracy of the classification reaches 95.73 %.24 **Keywords:** psychophysiological sensors; mental workload; Web browsing tasks; signal processing  
2526 

## 1. Introduction

27 Although Web applications are often justified in terms of increasing the productivity of human  
28 tasks, they sometimes have the opposite effect, interrupting, reducing the performance of, or  
29 increasing the mental workload of the user [1–4]. A typical task in which this phenomenon may  
30 occur is Web browsing. In this task, the user fixes her/his gaze on and between Web elements, i.e.,  
31 graphic or textual areas of a Web page, such as news, commercial advertisements, and menus [5–7].  
32 In cognitive psychology, mental workload refers to the total amount of perceived mental effort used  
33 for learning or processing new information [8–11].34 An important factor in measuring the effectiveness of a Web page is the user's browsing  
35 experience. It has been shown that the higher the level of user's browsing experience is, the lower the  
36 mental workload [3,4,12]. Every Web page has both an intrinsic and an extrinsic mental workload  
37 [3,13–15]. The former is related to the natural effort required to absorb new information, to the  
38 process of learning to navigate around the page, and to the process of becoming accustomed to the  
39 design of the page. The latter consists of the mental workload caused by the inclusion of unnecessary  
40 details or external interruptions, such as font styles that convey no meaning, commercial  
41 advertisement pop-ups, and irritating recommendations, which may have a negative effect on user's  
42 browsing experience.43 Continuously assessing, at any moment, the mental workload involved in browsing tasks  
44 entails measuring it either when the user fixes her attention on a Web element or when her gaze  
45 switches from one element to another. This assessment of mental workload can enhance the user's

46 browsing experience in many ways: for instance, avoiding extrinsic mental workload by  
47 automatically identifying the most suitable moments to proactively deliver content to the user or  
48 preventing irritating intrusions from the environment; reducing intrinsic mental workload by  
49 keeping the Web page support interventions on stand-by and adapting graphic user interfaces in  
50 real time; and evaluating the likelihood of user's abandonment, frustration or techno stress, among  
51 other benefits. In addition, instantaneous classification of mental workload into intrinsic or extrinsic  
52 to the Web elements of a Web page would make it possible to detect short time windows of reduced  
53 cognitive burden to activate the delivery of different types of recommendations in a timely,  
54 unobtrusive manner, such as contextual news in newspaper portals or commercial advertisement  
55 pop-ups on various Web sites. In addition, it may be possible to enhance search tasks, for instance,  
56 for restaurants, flight tickets, or retail products, by providing relevant feedback to the search engine  
57 based on the user's cognitive status [6].

58 To realize the above requirements, it is essential to address the challenge of automatically  
59 assessing the mental workload in a continuous fashion while the user is engaged in browsing, that is,  
60 in real time, with high frequency and using very short time windows.

61 Many studies have focused on classifying mental workload in general by capturing and  
62 processing data using ever less invasive psychophysiological sensors [16–20]. This method is  
63 founded on the empirical demonstration of the correlation existing between psychological stimuli  
64 and physiological responses triggered by the nervous system. Moreover, mental workload has been  
65 shown to vary frequently within a short time span [21,22].

66 Although considerable research has been devoted to assessing mental workload on the scale of  
67 hours and minutes by using data extracted from psychophysiological sensors, less attention has  
68 been paid to time windows lasting seconds or less, such as when a user fixes her gaze on a Web  
69 element. Indeed, Bailey et al. [23] have recently proved that moments of reduced mental workload  
70 occur while the user's attention is transiting from one task to another. However, this was shown only  
71 for coarse-grained tasks, such as selecting a travel route among alternatives presented in a graphic  
72 interface or classifying a list of emails into various categories [23].

73 In this paper, the capabilities of psychophysiological sensors are leveraged to research the  
74 possibility of assessing mental workload in real time during a browsing task. This paper thus  
75 attempts to answer the following research questions:

76

- 77 • RQ1: Is it possible to identify levels with regard to a user's mental workload within very short  
78 time windows (order of milliseconds) based on psychophysiological signals recorded during a  
79 Web browsing task?
- 80 • RQ2: Is it possible to accurately classify in real time a user's mental workload, both when her gaze  
81 is fixed on a Web element and when her gaze is transiting from one Web element to another, by  
82 combining different non-invasive psychophysiological sensors?

83

84 In addition, based on the findings of Bailey et al. [23], this paper attempts to prove the following  
85 hypothesis:

86

- 87 • H1: Mental workload is significantly smaller when the user's attention is switching from one Web  
88 element to another than when she is focused on a Web element.

89

90 To answer these research questions and prove the stated hypothesis, an experiment was  
91 conducted in which 61 users performed a normal Web browsing task in front of a computer screen  
92 while their psychophysiological responses were measured by different sensors and recorded in a  
93 database. The gold standard with regard to answering RQ1 is pupil diameter because several  
94 previous studies have shown that, under controlled illumination conditions, this  
95 psychophysiological response is a valid and reliable indicator of mental workload [23–29]. Using  
96 clustering methods, this paper shows that, by processing the pupil dilation response, four levels of  
97 mental workload can be identified per user on average.

98        However, measuring pupil dilation with an eye tracker is not a realistic and practical method to  
99        classify mental workload, for example, in the open air, because it requires constant and controlled  
100       illumination conditions. Thus, in this paper, more practical and less invasive sensors are assessed to  
101       measure other psychophysiological responses, such as heart rate (HR), electrodermal activity (EDA),  
102       body temperature, and electrocardiogram (ECG). The electroencephalogram (EEG) sensor is also  
103       assessed because there have been important advances in the construction of portable EEGs and in  
104       algorithms to reduce motion-related artifacts [30] [31]. It is expected that before long, there will be  
105       EEG devices that only capture brain waves from the areas of the brain relevant to the assessment of  
106       mental workload, making them less invasive [32].

107       This paper shows that, using all the sensors and efficiently processing their signals using  
108       artificial neural networks, mental workload can be classified as proposed in RQ2, with 68.94 %  
109       accuracy, 66.62 % recall, and 76.92 % precision. However, using all the sensors and a multi-layer  
110       perceptron, it is possible to achieve 88.46 % accuracy, 88.84 % recall, and 88.85 % precision.  
111       Ultimately, the best performance is obtained by combining EDA, HR, and EEG, achieving 95.73 %  
112       accuracy, 94.25 % recall, and 95.6 % precision in the classification of mental workload. Furthermore,  
113       the hypothesis that mental workload is significantly smaller when the user's attention is switching  
114       from one Web element to another than when she is focused on a Web element is confirmed  
115       ( $MSE = 1.7829$ ;  $p - value = 0.00184 < 0.05$ ).

116       The contributions of this paper include (i) identifying different levels of mental workload  
117       required for Web browsing through the processing and analysis of pupil dilation measured by an  
118       eye-tracking sensor; (ii) developing a method for appropriately combining non-invasive  
119       psychophysiological sensors to classify real-time mental workload in small time windows with high  
120       accuracy (mean=99.1%, SD = 0.2772%) based on the behavior of the user's gaze in a Web browsing  
121       task; and (iii) leaving open the possibility of using gaze shifts from one Web element to another as  
122       the most appropriate time to provide the user with recommendations, for example.

123       This paper is organized as follows. Section 2 provides the background required to understand  
124       this research. Section 3 presents the related literature. The experiment conducted is described in  
125       Section 4, as well as the data processing and the machine learning methods applied to the data. The  
126       results are presented in Section 5 and are discussed in Section 6, while Section 7 concludes the paper.

## 127       2. Background

### 128       2.1 Assessment Methods

129       Cognitive resources are assets used by cognition to think, remember, make decisions, solve  
130       problems, or coordinate movements, such as perception, attention, short- and long-term memory,  
131       and motor control [33,34]. According to Navon et al. [35], these resources underlying human  
132       learning and information processing are limited [36].

133       Wickens [9], in his multiple resource theory, suggests that these resources can be used in  
134       parallel for multiple tasks, using several resources at once. However, when task demand is high, the  
135       resources allocated to that task are not available for another task if the same mental resources are  
136       required at the same stage of processing. Excessive use, moreover, can cause a state of overload  
137       known as cognitive resource depletion [37]. This overload means that the brain is unable to process  
138       new information, resulting in processing and/or execution errors [38].

139       Mental workload results from the different levels of resource demand, depending on the  
140       parallel tasks that the person is performing [8,9,21,22]. Excessive resource demand can cause  
141       distraction, increase errors, generate stress and frustration, and reduce the ability to undertake  
142       mental planning, problem solving, or decision-making [39,40]. One example is the distraction caused  
143       by unwelcome advertisements on a Web page while the user is browsing. In this case, the  
144       intermingling of the browsing task with the intrusion of commercial advertisements forces the user  
145       to divide attention and allocate cognitive resources to the new stimulus.

146       Traditionally, mental workload has been assessed in different situations using subjective  
147       methods [16] based on surveys, auto-perception scales, or think-aloud protocols [41–43]. These

148 methods are applied after the user has already finished the task, and the assessment of the mental  
149 workload depends of the user's final perception [44]. Therefore, these methods are constrained by  
150 the reporting bias introduced by relying on past memories and by the problem of ecological validity  
151 based on observing responses to hypothetical scenarios rather than behaviors in a real setting [45]. In  
152 addition, the static nature of these methods makes them unfit for real-time evaluation. The most  
153 widespread example of this method is the NASA Task Load Index, which measures the mental and  
154 physical performance, as well as the effort and frustration, of the user [46].

155 Performance-based methods have also been used, which measure indicators generated during  
156 task execution, such as the percentage of correct responses or execution time [3,16,17]. In this  
157 method, the user needs to be engaged in only one task. Its major restriction is the difficulty of  
158 assessing mental workload in near real time.

159 The attempts to find objective indicators to measure mental workload in real time are based on  
160 collecting contextual information, which can be captured mainly using psychophysiological sensors  
161 [47–49]. Indeed, there is ample empirical evidence in psychophysiology showing that some  
162 physiological responses are directly related to psychological factors such as stress, mental workload,  
163 and emotions [50–52]. That is, there is a correlation between the physiological responses triggered by  
164 the nervous system and psychological stimuli.

165 Psychophysiological responses are controlled by the autonomic nervous system (ANS), which  
166 regulates and coordinates bodily processes such as digestion, temperature, blood pressure, and  
167 many aspects of emotional behavior [53]. These actions occur independently of the conscious control  
168 of the individual. The ANS includes the sympathetic nervous system (SNS) and parasympathetic  
169 nervous system (PNS). The SNS controls actions required in emergency situations, such as stress and  
170 movement. It can cause heart rate acceleration, pupil dilation, and increased blood flow to the  
171 muscles, sweating, and muscle tension. The PNS controls the functions related to rest, repair, and  
172 relaxation of the body. The responses elicited by this system include a decrease in heart rate and  
173 blood pressure, stimulation of the digestive system, and pupillary contraction, among others [50,51].

## 174 2.2 *Psychophysiological measurements*

175 There are different types of methods to measure psychophysiological responses elicited  
176 complementarily by the SNS and PNS [54]. For instance, the device for tracking gaze is the eye  
177 tracker. It consists of a camera on the computer screen that works according to the "corneal-reflection  
178 / pupil-center" method [55]. It also allows the measurement of the variation of the pupil diameter.  
179 The pupillometry measures changes in pupil size, which can be attributed to both parasympathetic  
180 inhibition, which explains the first dilation phase, and sympathetic activation, which explains the  
181 subsequent contraction phase [56,57]. Although pupil dilation can be triggered by a light reflex  
182 caused by changes in environment illumination or by a proximity or accommodation reflex to  
183 improve visual focus, it can also be caused by a psychosensory reflex associated with the cognitive  
184 or emotional engagement of the person while exposed to any sensory stimulus [58]. In contrast to  
185 changes in the two previous reflexes, changes in pupil size in this case are subtler, so a  
186 high-precision device or eye tracker is required for their detection [59].

187 The eye tracker is also used for tracking the eye to determine gaze position or movements  
188 within a scene, including two relevant measurements:

189

- 190 • *Fixations*: moments during which the gaze is relatively fixed or focused. They occur because  
191 sharp vision is only possible within a small area in the human eye called the fovea. It is useful to  
192 determine when eye fixation occurs because, in most cases, it coincides with attention.
- 193 • *Saccades*: rapid eye movements or jumps from one fixation point to another. Saccades follow a  
194 pattern (or trajectory) depending on several factors: what is currently being looked at, visual  
195 target tracking, experience, and emotions.

196  
197 Another set of psychophysiological measurements is obtained by electroencephalography. This  
198 is based on recording the electrical activity of the brain measured on the scalp. The device used is the

199 EEG, which measures the voltage resulting from changes in ionic current flow within the neurons of  
200 the brain, produced by the brain's synaptic activity. There are five major brain waves: delta (1-4 Hz),  
201 theta (4-8 Hz), alpha (8-12 Hz), beta (12-25 Hz), and gamma (approximately 25 Hz). Fritz et al. [16]  
202 indicate that a decrease in the activity of the alpha band in conjunction with an increase in the  
203 activity of the theta band is associated with greater attentional demand and memory workload.  
204 Moreover, other studies have concluded that theta and delta bands are sensitive to stimuli involving  
205 difficult manipulation.

206 EDA is a psychophysiological response that can be assessed by measuring changes in the  
207 electrical properties of the skin. Skin conductivity varies with changes in skin moisture (sweat) and  
208 may reveal changes in the SNS. EDA is also known as galvanic skin response (GSR), and it is  
209 inexpensive to assess, easily captured, and robust. It is measured by attaching one or two electrodes  
210 usually to the fingers or toes. It is an indicator of psychological and physiological arousal. In  
211 addition, it serves to identify emotional states. EDA has two components: (1) a phasic component  
212 that changes rapidly and is related to external stimuli or a non-specific activity and (2) a tonic  
213 component or base signal that varies slowly and sets basic skin conductance. A classic behavior is  
214 that when arousal increases, there is an increase in sweat gland activity, decreasing electrical  
215 resistance, and thus increasing conductivity.

216 The cardiovascular system is particularly interesting for psychophysiology because it is highly  
217 sensitive to neurological processes and psychological factors such as stress. It is regulated by the  
218 ANS, which produces patterns of electrical activity that are fundamental for psychophysiological  
219 measurements [50]. Several studies associate changes in cardiac activity with psychological  
220 phenomena, such as mental work, perception, attention, problem solving, and signal detection [60].

221 An ECG is used to measure the electrical activity of the heart, using at least three electrodes  
222 attached to the chest. The electrodes collect the necessary data with regard to the electric waves that  
223 describe the cardiac cycle, based on which the HR or its variation (HRV) are obtained.

224 The human body constantly exchanges heat with the environment as part of the process of  
225 self-regulation to maintain homeostasis (internal balance of the body). Body temperature increases  
226 and decreases in relation to the energy exchanged. The regulation of blood flow to the skin and  
227 thermal radiation is considered a function of the ANS [61]. Studies conducted in this field, according  
228 to Genno et al. (1997) [62], suggest that skin temperature has potential as a psychophysiological  
229 measure of the individual.

### 230 3. Literature Review

231 This paper focuses on the measurement of mental workload while the user browses a Web site  
232 in front of her personal computer. However, the literature in this regard is scant. Thus, to start  
233 studying the measurement of mental workloads in various domains and to help understand the  
234 methodology associated with this type of research, this section focuses on two main points: the  
235 assessment of mental workload using psychophysiological sensors in general and the measurement  
236 of mental workload in Web environments.

#### 237 3.1 Assessment of Mental Workload with Psychophysiological Sensors

238 A relevant study for this paper is that by Bailey et al. [23] who develop psychophysiological  
239 measures to assess the effect of interruptions on the performance of a person executing a task. They  
240 establish that interruption involves considerable negative effects, such as increased time to complete  
241 the task [63], a wider range of errors [64], additional efforts in decision-making [65] and mood  
242 changes such as increased frustration and anxiety [66–68]. For example, when an interruption occurs  
243 at a random time while performing a major task, the time to completion can increase by up to 30 %,  
244 up to twice as many errors can be committed, and user displeasure doubles, in contrast to when the  
245 interruption occurs at a pre-programmed time. Therefore, Bailey et al. empirically find that  
246 interruptions may have a lower cost if they occur at a time of low mental workload, hypothesizing  
247 that this may occur at the boundaries between subtasks when executing the general task [69]. As a  
248 test method, they assess mental workload by pupil dilation in three different tasks that include

249 respective subtasks. The first task consists of assessing two different routes between two cities on a  
250 monitor; the user must measure the distance and cost of the routes, tabulate the data, and, finally,  
251 discriminate and choose the shortest and most economical route. In the second task, the user must  
252 edit a document and correct spelling at three levels of complexity (editing a word, editing two  
253 words, and editing a complete sentence). The third task entails classifying nine emails involving  
254 explicit issues (low complexity) and ambiguous issues (high complexity) into four categories. Each  
255 of these scenarios is applied to 24 people (seven women) between 19 and 50 years of age. The main  
256 conclusions of the study are as follows: (i) mental workload varies during the execution of the three  
257 tasks, (ii) the mental workload decreases when performing subtasks compared to the general task,  
258 and (iii) different subtasks demand different levels of mental workload based on their complexity.

259 Other studies focus on training classifiers to process psychophysiological signal data in a time  
260 window in order to predict whether the load associated with a specific task is high or low [70]. For  
261 example, Haapalainen et al. [17] measure the mental workloads of basic tasks such as the resolution  
262 of problems on a monitor, visual perception, and cognitive speed by using an eye-tracking device,  
263 EEG, ECG, heat flow, and rate measurements. As a result, they find that ECG and heat flow together  
264 distinguish between tasks of high and low cognitive demand with 80 % precision.

265 Fritz et al. [16] seek to verify whether psychophysiological sensors are useful in measuring the  
266 difficulty of a computer code comprehension task with various levels of difficulty. The tasks are  
267 performed by software developers, who are monitored using an eye tracker and an  
268 electroencephalogram. Fritz et al. use the *Beta/(Alpha + Theta)* ratio based on the evidence that  
269 beta increases with task execution, theta is deleted, and alpha is blocked. The models obtained  
270 classify task difficulty with 85 % accuracy.

271 Shi et al. [71] assess stress and arousal levels by measuring EDA for increasing levels of  
272 difficulty. The experiment consists of a transition interface in which the participants must respond to  
273 the requirements in three scenarios: (1) using gestures and speaking, (2) only speaking, and (3) only  
274 using gestures. The difficulty varies depending on level of visual complexity, number of entities,  
275 number of distractors, time limit, and number of actions to complete. The results indicate that there  
276 is a significant increase in the EDA signal as task difficulty increases.

277 Nourbakhsh et al. [72] confirm the effectiveness of EDA in discriminating between the difficulty  
278 of eight arithmetic tasks with four levels of difficulty. In addition, as an extension of the previous  
279 study, Nourbakhsh et al. measure mental workload using EDA changes and the number of blinks  
280 obtained from an eye-tracking device. The experiment is the same as in the previous study. This  
281 time, by combining both sensors, 75 % precision is achieved for the lowest level of difficulty.

282 Xu et al. [73] show that mental workload can be measured by pupil dilation if illumination  
283 changes. The experiment consists of arithmetic tasks that vary in difficulty depending on the  
284 number of digits.

285 In Ikehara et al. [18], an eye-tracking device, a pressure sensor for the mouse, an EDA sensor,  
286 and a pulse oximeter (for measuring HR and level of oxygen in the blood) are used. The experiment  
287 consists of selecting on a screen the fractions whose value is less than 1/3. There are two levels of  
288 difficulty in the experiment. The results indicate that EDA and pupil dilation have the greatest  
289 statistical significance in terms of detecting task difficulty.

290 Using an elastic neural network, Hogervost et al. [19] find that the best performance is obtained  
291 when EEG is combined with pupil dilation (91% accuracy) and when EEG is combined with  
292 peripheral physiology (89 %); with EEG alone, they obtain 86 % accuracy. In addition, using only the  
293 measurement of the electrode located in the Pz position (central parietal area of the head), they  
294 obtain 88 % accuracy.

### 295 3.2 Assessment of Mental Workload in Web Environments

296 Although the study of users' cognitive responses during Web browsing is an intriguing area, it  
297 remains little explored. Indeed, one of the few studies on the topic is that by Albers [3], who  
298 examines how mental workload theory applies to the design of Web sites using the tapping test  
299 method, which measures mental workload by focusing on performance. As in all the examples using

300 this approach, the tapping test adds an additional secondary task to the main one, measuring the  
301 performance of the participant to determine the level of mental workload induced. In this case, the  
302 main task is to browse two Web sites sequentially—with implicit mental workload controlled by  
303 design—and answer questions aloud in relation to the Web pages, while the secondary task is to  
304 rhythmically keep tapping per second. As mental workload increases, tapping begins to fall slowly  
305 and lose the rhythm, even losing it completely when there is cognitive overload. However,  
306 implementing a secondary task as required by this method prevents from generating a realistic  
307 scenario for the user and does not allow real-time measurement.

308 The most recent research regarding the observation of Web users' experience involves the  
309 measurement of their behavior as a reaction to different stimuli, such as notifications, and allows us  
310 to predict the user's response according to Navalpakkam & Churchill [74]. By comparing mouse  
311 pointer movement to eye tracking, they are able to determine a more user-friendly layout for a Web  
312 site, which improves the effectiveness of the notification. Finally, they conclude that gaze and mouse  
313 movement patterns contain important information in terms of assessing the user's status,  
314 determining if they are distracted from the assigned task or striving to fulfill it. The correlation  
315 between eye movements and mouse pointer movement predicts a Web user's different  
316 psycho-emotional states. They also conclude that the user is more likely to pay attention to  
317 notifications when they vary in position on the Web site rather than when they are fixed.

318 As summarized in Table 1, the measurement of mental workload using psychophysiological  
319 signals has been tested for a varied set of tasks. In addition, studies have investigated how mental  
320 workload is related to the design of a Web page. However, the abovementioned research provides  
321 no evidence regarding assessment of mental workload while browsing a Web site using multiple  
322 psychophysiological measures. There is also no reference to time overhead to determine how  
323 feasible it is to implement real-time measurement. Partial. Time Windows average length for classification  
324 of 23.7 s.

## 325 4. Materials and Methods

### 326 4.1 Participants

327 The initial experimental group includes 61 participants (19 women and 42 men), aged between  
328 19 and 35 years (*mean age* = 23.8 years, *SD* = 3.2 years), all engineering students at the University of  
329 Chile, recruited through the institutional news Web application. None of them suffered from  
330 cardiovascular diseases or was taking medications that could have affected their normal behavior.  
331 All of them were familiar with browsing tasks. Each session had a duration of approximately 60 min.  
332 The final experimental group is composed of 53 people. Eight participants were discarded due to  
333 various problems during signal measurement and processing.

334 This research has the approval of the Research Ethics Committee at the Faculty of Physical and  
335 Mathematical Sciences at the University of Chile. In addition, all of the participants read an informed  
336 consent and agreed on signing it. The consent contained information about the procedure, purpose  
337 of the experiments, voluntary participation, right to decline to participate at any moment, how to  
338 access the research results and researchers' information.

### 339 4.2 Psychophysiological Sensors

340 Psychophysiological sensors have the advantage that measurements do not depend on the  
341 user's perception and are not under the control of the user.

342

**Table 1.** Related work analysis

Ref.	Small Time Windows	Real Time	Web Browsing Tasks	Multiple Psychophysiological Sensors
[15]	Partial. Time window average length for classification of 23.7 s.	Fulfils	Fails. Desktop-based tasks of visual perception and cognitive speed.	Fulfils. Eye tracker, EEG, ECG, heat flux and HR.
[14]	Partial. Sliding time windows of sizes from 5 seconds to 60 seconds, sliding 5 seconds between intervals.	Fulfils	Fails. Comprehension tasks of computer code.	Fulfils. Eye tracker, EEG
[34], [37]	Partial. Three silent reading tasks were performed. Each task consisted of four text slides and each slide was presented for 30 seconds.	Fulfils	Fails. Arithmetic tasks	Partial. EDA and blink.
[16]	Fails. Duration of tasks between 60 and 70 seconds.	Fulfils	Fails. Select the fraction whose value is less than 1/3.	Fulfils. Eye tracker, EDA, pulse-oximeter, mouse pressure sensor.
[17]	Fails. Classification in 2 minutes windows.	Fulfils	Fails. N-back task.	Fulfils. EEG; peripherals (EDA, respiration, ECG) and eye measures (eye tracker).
[18]	Fulfils. The average overall duration of the limits was 550 ms.	Fulfils	Partial. Measures the cost of interruptions in tasks such as: choosing a route, correcting spelling and classifying emails.	Partial. Only the pupillary dilation.
[3]	Not applicable.	Fails	Fulfils. Measure the cognitive load on a website.	Fails. Measurement of mental workload by performance: tapping test.
[36]	Fails. The participants interacted with each page for about 100-120 seconds.	Fulfils	Fulfils. Study the design of websites in a way that improves the effect of a notification.	Partial. Compare the tracking of the mouse with eye tracking.
[38]	Fulfils. Windows between 300 and 600 ms.	Fulfils	Fulfils. Predict the intention of clicking on a website.	Partial. Only the pupillary dilation.

In addition, they are becoming less intrusive and allow tasks to be performed in various scenarios, giving greater ecological validity to the experiments. They also allow real-time data capture [16,50].



348

349 **Figure 1.** Participant with the sensors runs the experiment. The sensors are: (1) ECG, (2) axillary  
350 temperature, (3) EEG, (4) EDA, (5) PPG and (6) eye tracker.

351

352 For data acquisition, the following sensors were used: GSR+, optical pulse sensor, and Bridge  
353 Amplifier + unit, all from the Shimmer [75]; ECG BITalino [76]; EEG Emotiv EPOC [77]; and Tobii  
354 T120 Eye Tracker [78]. Figure 1 shows an example of a volunteer outfitted with all the sensors.

355 To measure the EDA and HR signals, the Shimmer GSR+ unit sensor was used with a sampling  
356 frequency of 120 Hz. The position of the electrodes for measuring the EDA was the palm area of the  
357 proximal phalanx of the index and ring fingers of the left hand [79]. The optical sensor that functions  
358 as a photoplethysmograph (PPG) was attached to the lobe of the right ear [80]. The Shimmer Bridge  
359 Amplifier + unit sensor with a sampling frequency of 50 Hz was used to measure body temperature.  
360 The sensor was applied under the right armpit. This sensor was synchronized with the EDA and  
361 pulse sensors using a base provided by Shimmer together with Consensys software.

362 The BITalino BioMedical Development All-in-One Board with a sampling frequency of 1000 Hz  
363 was used to measure the ECG. The configuration of the three electrodes followed the lead II  
364 standard [81,82]. Before applying the electrodes, the skin was prepared by wiping it with alcohol to  
365 remove grease and impurities to reduce noise. In addition, an ECG gel was used. OpenSignals  
366 evolution software provided by the manufacturer was used [83].

367 To measure the EEG, the Emotiv EPOC EEG sensor with a sampling frequency of 128 Hz was  
368 used. The sensor was attached to the head, positioning the reference sensors first. To improve the  
369 conduction of the electrical signals of the brain, each electrode was previously hydrated. To capture  
370 the data and verify that the sensor was properly applied, the Emotiv Xavier Testbench software  
371 provided by the manufacturer was used.

372 The Tobii T120 Eye Tracker with a sampling frequency of 120 Hz was used to measure pupil  
373 dilation and for eye tracking. Tobii Studio software was used for calibration and to perform data  
374 collection [84]-

#### 375 4.3 Experimental Procedure

376 A fictitious Web site was created whose basic configuration is shown in Figure 2. This layout of  
377 the Web elements was maintained through all the experiment. The elements within the Web site  
378 were seven news headings with their respective representative image, four rectangular  
379 advertisements, a typical navigation bar with a menu, the logo of the page in the upper left corner,  
380 and a bar at the bottom of the page.

381

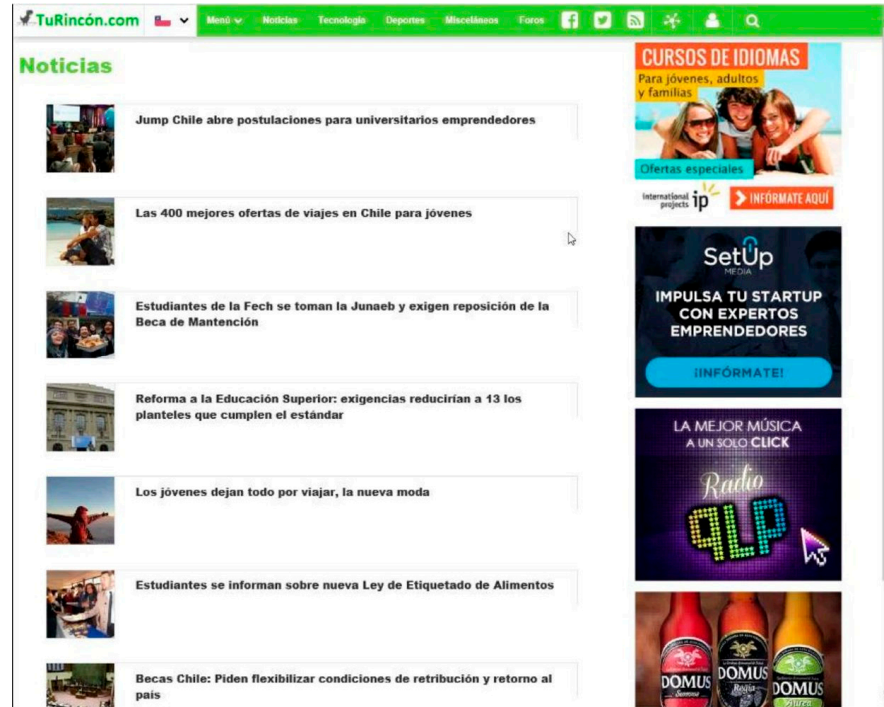


Figure 2. Example of a dummy Web page for the experiment.

382

383

384

385 Each participant was tested individually at the laboratory. A physically isolated experimental  
 386 room was used to maintain the experimental configuration and the environment constant for all  
 387 participants. In addition, the room did not receive any sunlight, to avoid the effects of infrared light  
 388 on measurements and to maintain constant illumination conditions that do not affect pupil diameter  
 389 measurements [85].

390 As soon as the participant arrived in the experimental room, the experiment was explained to  
 391 her, and she was asked to read and sign the informed consent, as well as a questionnaire to get her  
 392 basic anonymous information. The participant seated in front of the screen, and the sensors were  
 393 connected in the following order: ECG, axillary temperature, EEG, EDA, and PPG; then the eye  
 394 tracker was calibrated with the help of the participant (Figure 1).

395 Prior to the tests, each user underwent a relaxation period consisting of the visualization of  
 396 three four-minute videos of landscapes with background instrumental music. Then, the participant  
 397 was asked to take deep breaths for one minute with eyes closed and with soft background  
 398 instrumental music. This procedure aimed to eliminate the Hawthorne effect – modification in the  
 399 behavior of the subjects due to their awareness of being studied – and physiological effects similar to  
 400 the "white coat" effect in measured signals [86]. Next, the participant was asked to maintain a fixed  
 401 posture, sitting in front of the computer, without moving the head or the left hand, where the  
 402 sensors were connected. The instructions were that the user could freely browse the Web site for as  
 403 long as they wanted and indicate when they wanted to finish. Finally, all sensors were removed  
 404 from the participant, while she was asked do not tell others the experimental procedure.

405 4.4 Data Analysis

406 4.4.1 Time Window Definition

407 Bailey (2008) [23] shows that mental workload decreases during transitions between subtasks.  
 408 For this paper, the analysis of each Web element is considered a specific subtask and the passage  
 409 between them as the transition period between subtasks. Thus, in this study, mental workload is  
 410 assessed during two time windows:

411

412

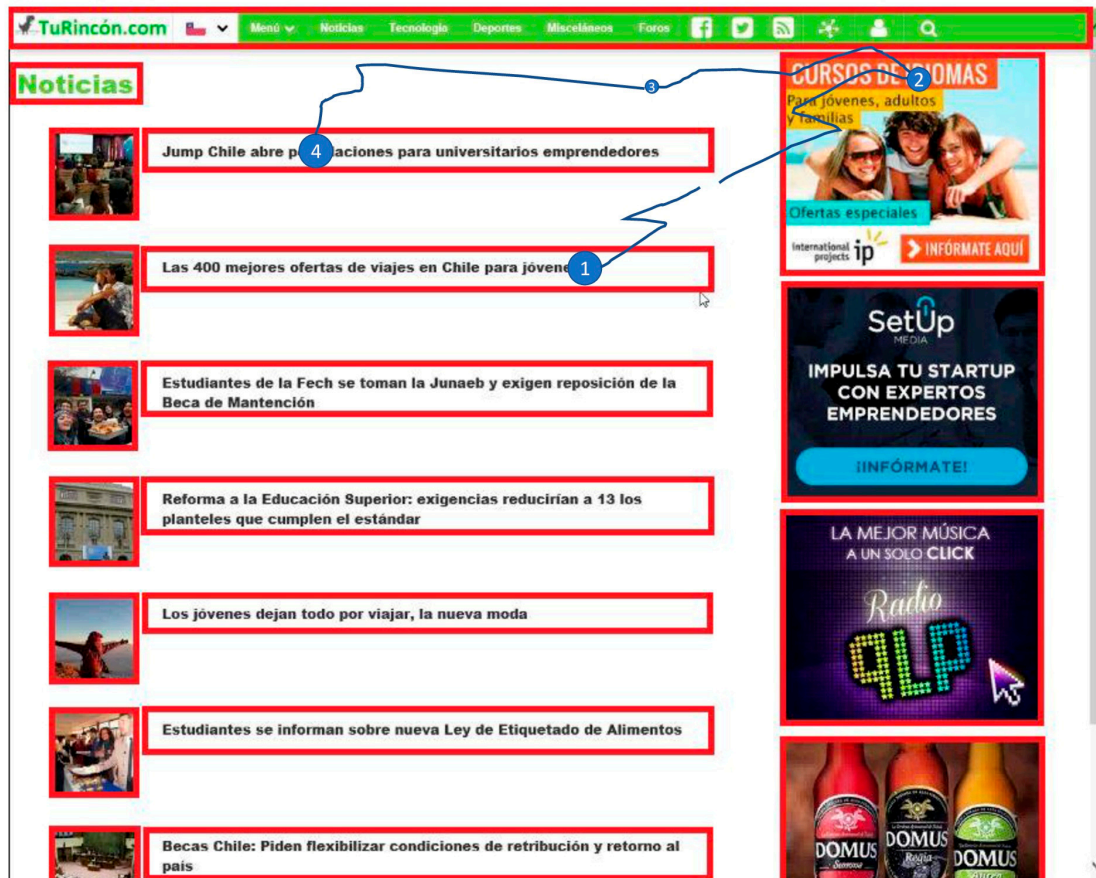


Figure 3. Example of active window and transition window.

- *Active window*: Time during which the user fixes her gaze on a specific area of interest (AoI), which may correspond to a news headline, an advertisement, or the menu bar of the Web site.
- *Transition window*: Time that elapses while the user is not fixing her gaze on any of the areas of interest. It can be a transition between two elements or towards the same element.

As illustrated in Figure 3, the red rectangles represent the studied AoIs; the blue circles represent fixations, which size varies in accordance with the fixation time and the blue lines represent the saccades. Thus, the time a fixation is into an AoI pertains to an active window. The time between two fixations, such as fixation one and fixation two, pertains to a transition window. Note that the transition window between fixation two and four add the fixation three, which does not fall into any AoI.

To discriminate between types of windows, the data file exported from the Tobii Studio program generates a column showing the AoI that the participant is inspecting for each sample. It discriminates between 3 values: when the user is not looking at the screen – inactive –, when the user is looking at a certain AoI – active window –, and when the user's gaze is directed outside the AoI – which is considered a transition window.

A long minimum time of 500 milliseconds is set to define a valid time window. This is based on the research of Loyola et al. [87], who assesses the identification of key Web elements in a Web site using eye tracking. This time span is selected to avoid possible contamination of the pupil signal by the analysis of a previous object. Time windows below the threshold are not considered for analysis and are therefore deleted. When the same Web element is analyzed before and after a deleted window, the two segments are joined, generating a window of greater length.

413

414

415

416

417

418

419

420

421

422

423

424

425

426

427

428

429

430

431

432

433

434

435

436

437

438

439

440

## 441 4.4.2 Data Preprocessing

442 The data exported from Tobii Studio contains the diameter of the left pupil, the diameter of the  
 443 right pupil (both in millimeters), and the validation of the reliability of the capture of each pupil  
 444 between 0 – high reliability – and four – the eye was not detected. On average for all participants and  
 445 considering only valid windows, the reliability of the capture of the left pupil is 0.2469, and that of  
 446 the right pupil is 0.22036; these are reliable values to validate the capture of pupil diameter data. As  
 447 these values are an average for all the participants, the pupil data with the highest level of reliability  
 448 are selected for each sample [16].

449 Next, signal distortion artifacts, such as saccades and blinks, are eliminated. A column in the  
 450 extracted data shows if the sample is a fixation or a saccade, and this information is used to filter  
 451 saccades. Furthermore, a linear interpolation between the values of the blinks detected is used. In  
 452 addition, a Blackman window with a cut-off frequency of 2 Hz is applied as a low-pass filter.

453 EDA raw data provides the values of electric resistance of the skin in Kilohms [ $k\Omega$ ]. To reduce  
 454 noise and eliminate motion artifacts, two procedures are performed: first, a strict instruction is given  
 455 to each participant not to move the hand or fingers where the electrodes are attached, and second,  
 456 the signal is filtered with a low-pass cut-off frequency of 5 Hz. Furthermore, on the recommendation  
 457 of the literature [88], capture resolution is reduced without risk of data loss. The EDA signal  
 458 measured with a sampling frequency of 120 Hz is reduced to 10 samples per second. The phasic  
 459 component is extracted by applying a median filter with a window width of -4/+4 and subtracting  
 460 the average of the current sample [88]. This component allows the detection of peaks of the EDA  
 461 signal. With slow transitions, the phasic component does not show major variations.

462 Regarding the electrocardiogram, the raw data yield values that must be transformed to  
 463 millivolts [mV]. The processing of this signal consists of using a low-pass filter with a cut-off  
 464 frequency of 100 Hz and applying the fast Fourier transform to obtain the characteristic shape.

465 The raw data of the PPG yield signal values in millivolts [mV]. From this signal, it is possible to  
 466 obtain the HR. Previously, the PPG signal is processed using a low-pass filter with a cut-off  
 467 frequency of 16 Hz with a Blackman window, obtaining a cleaner signal. Then, HR is obtained via  
 468 the following steps: first, the peaks must be found; second, the time between them is subtracted ( $\Delta t$   
 469 in [milliseconds / pulse]); third, they are converted from hundredths to seconds and from [seconds /  
 470 pulse] to [pulses / second], which is then multiplied by 60 to convert to [beats/minute]. This is  
 471 resume in the Equation (1):

$$472 \quad HR = \frac{60}{\Delta t \cdot 100} \left[ \frac{\text{beats}}{\text{minute}} \right] \quad (1).$$

473

474 The raw data yield body temperature values in degrees Celsius. The processing of this signal  
 475 consists of using a low-pass filter with a cut-off frequency of 1 Hz, as concluded based on the data  
 476 collection in Haapalainen et al. [17].

477 The EEG signal is subject to a wide variety of artifacts and noise [89,90]. Among the elements  
 478 that cause artifacts are blinking, oculomotor activity, head movements, facial expressions that add  
 479 noise due to the muscle electrical signal, and movement of the electrodes, among others. To  
 480 eliminate the effect of head swinging, a high-pass filter with a cut-off frequency of 0.5 Hz is used. In  
 481 addition, a low-pass filter with a cut-off frequency of 40 Hz is used to eliminate noise from the  
 482 electrical grid (50 - 60 Hz). To eliminate outliers and decrease the effect of the blinking artifact a  
 483 Hampel filter is used [91].

## 483 4.4.3 Feature Extraction

484 Feature extraction is performed based on time windows. Since signals have different scales, to  
 485 be comparable objects, it is necessary to standardize them before extracting characteristics from  
 486 them, as proposed by Guyon et al. [92]. To perform standardization, the classical  $(x - \mu)/\sigma$  form is  
 487 used, where  $x$  is the vector corresponding to the signal, and  $\mu$  and  $\sigma$  are the mean and the  
 488 standard deviation of the signal, respectively.

489

490  
491**Table 2.** Characteristics extracted by each signal.

Signals	Extracted Characteristics
Pupil	mean, standard deviation
EDA	Accumulated data, average as a function of time and spectral power
Phasic	average, absolute value of the maximum, number of peaks
ECG	mean, median, variance of ECGMAD (average absolute deviation)
PPG(HR)	mean, standard deviation, RMS of HR
T	mean, median
EEG	power and phase of the analytical signal obtained with the Transf. of Hilbert

492  
493

494 A total of 44 characteristics pertaining to the different signals are extracted: two from pupil  
 495 dilation, six from EDA, two from body temperature, three from ECG, three from PPG-HR, and two  
 496 from each of the 14 EEG channels. Table 2 shows a summary of the characteristics, following which  
 497 the obtained characteristics are presented in more detail.

498 Because it has been proven that pupillary response is an important indicator of the mental effort  
 499 required to solve a task, it is selected as the gold standard by which to cluster windows and generate  
 500 labels for cognitive levels. There are clustering cases in the literature regarding the development of  
 501 Web tasks such as the study of Loyola et al. [87]. The selected characteristics are the mean and  
 502 variance of the pupil diameter of the eye that displays greater reliability in its measurement.

503 Based on the findings of Nourbakhsh [72] and Shi et al. [71], the following characteristics are  
 504 extracted from the processed EDA signal: accumulated normalized data, mean as a function of  
 505 normalized time, and spectral power without normalized continuous component. Equation (2)  
 506 shows the calculation of the normalized EDA signal. Each point in time  $t$  is added, where  $i$   
 507 corresponds to the participant,  $k$  and  $m$  is the total number of tasks;  $m = 3$  in this case:

508

$$EDA_{normalized}(i, k, t) = \frac{EDA(i, k, t)}{\frac{1}{m} \sum_{j=1}^m \sum_{t=1}^{T_{ij}} EDA(i, j, t)} \quad (2).$$

509

510 Therefore, the data for each participant are normalized by dividing the task signal by the mean  
 511 value of all the tasks for the subject. Then, the accumulated EDA characteristics are calculated as  
 512 shown in Equation (3) and mean EDA is calculated according to Equation (4), where  $T$  is the total  
 513 time for all the tasks:

514

$$EDA_{accumulated}(i, k) = \sum_t EDA_{normalized}(i, k, t) \quad (3),$$

515

516

$$EDA_{average}(i, k) = \frac{\sum_t EDA_{normalized}(i, k, t)}{T} \quad (4).$$

517

518

519 The following characteristics are extracted from the phasic component obtained: number of  
 520 peaks, maximum modulus, and average of the phasic component of the window [16].

521 Based on the proposal by Haapalainen et al. [17], the following characteristics are selected for  
 522 the ECG signal: median, mean, and variance of the ECG median absolute deviation (ECG\_MAD),  
 523 calculated using Equation (5):

524

$$ECG\_MAD = |ECG_i - median(ECG)| \quad (5).$$

525

526 The characteristics of the heart rate obtained from the PPG signal are selected based on the time  
527 domain characteristics used in Betella [93]. These are the mean, standard deviation, and root mean  
528 square of HR. Based on the proposal by Haapalainen et al. [17], the median and mean of the  
529 temperature are selected.

530 For the EEG signal, there are two main approaches: event-related potential (ERP) analysis and  
531 time-frequency signal analysis. The latter is selected because it is more closely related to the  
532 psychophysiological and structural processes of the brain [89]. It is used to study  
533 emotional-cognitive states in particular and is more advisable when studying a limited period or a  
534 relatively low amount of data, as is the case of the time-window study of this paper [94]. Among  
535 the different ways of analyzing the EEG signal in time-frequency are frequency bands with Fourier  
536 transform, Morlet wavelets, and Hilbert transform. All three show similar results according to  
537 Cohen [95]. Thus, the option of the Hilbert Transform ( $\mathcal{H}\{eeg\}(t)$ ) is selected, which has the  
538 advantage of greater control over frequency filtering. The Equation (6) shows this transform:  
539

$$\widehat{eeg} = \mathcal{H}\{eeg\}(t) = (h * eeg)(t) = \frac{1}{\pi} \int_{-\infty}^{\infty} \frac{eeg(\tau)}{t - \tau} d\tau \quad (6),$$

540

541 where  $h(t) = 1/\pi t$ ,  $eeg$  is the EEG signal and  $\widehat{eeg}$  is the resulting analytic signal. Before applying  
542 this transform, a bandpass filter between 2 and 15 Hz is used to center the study in the theta (4 - 8  
543 Hz) and alpha (8 - 12 Hz) frequency bands. These are related to states of mental activity and  
544 relaxation, respectively, where theta increases and alpha is suppressed when there is mental  
545 workload [94]. A complex signal called the "analytical signal" is then obtained, from which two  
546 characteristics are extracted. This is performed for each of the 14 channels of the EEG signal.

#### 547 4.4.4 Clustering

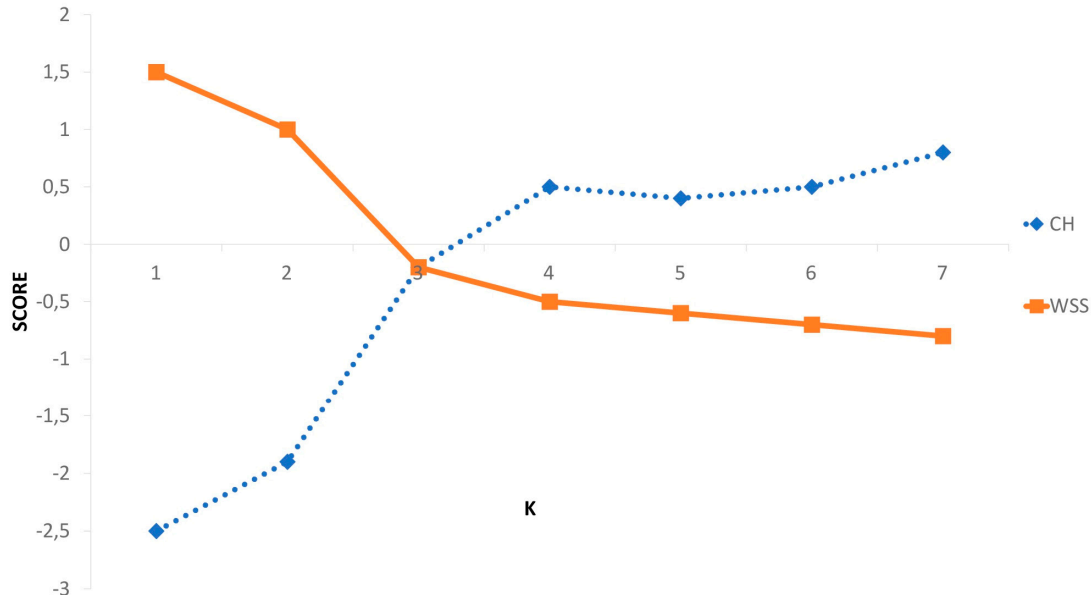
548 Clustering is performed per participant to determine how many levels of mental workload the  
549 user presents based on the measurement of pupil diameter in order to label the database after  
550 ascertaining these levels. In Loyola et al. [87], the k-means method is used. Because an  
551 overestimation or underestimation of the number  $K$  of clusters affects the quality of the cluster, the  
552 optimal value of clusters is sought. The  $K$  value is tested from two onwards to obtain two curves.  
553 The index of Calinski & Harabasz (CH) and the internal measure of cohesion of the sum of the  
554 squares within the group (WSS) are selected to this end [96–98]. The stop rule is the value closest to  
555 the area where the curves interact. Figure 4 shows an example of this methodology for participant  
556 59, where the intersection is generated at  $K = 3$ . Visually, the grouping can be validated considering  
557 Figure 5.

558 The Jaccard coefficient obtained using the bootstrap method is used as an external criterion for  
559 validating clusters, which assesses how stable the cluster is [96,97]. Values between 0.6 and 0.75  
560 indicate that the group is measuring a pattern in the data, but there is no certainty as to which points  
561 should be grouped. Groups with stability values above approximately 0.85 can be considered highly  
562 stable (real clusters). There are participants who present well-defined clusters with Jaccard  
563 coefficients very close to one, and others with values far from acceptable.

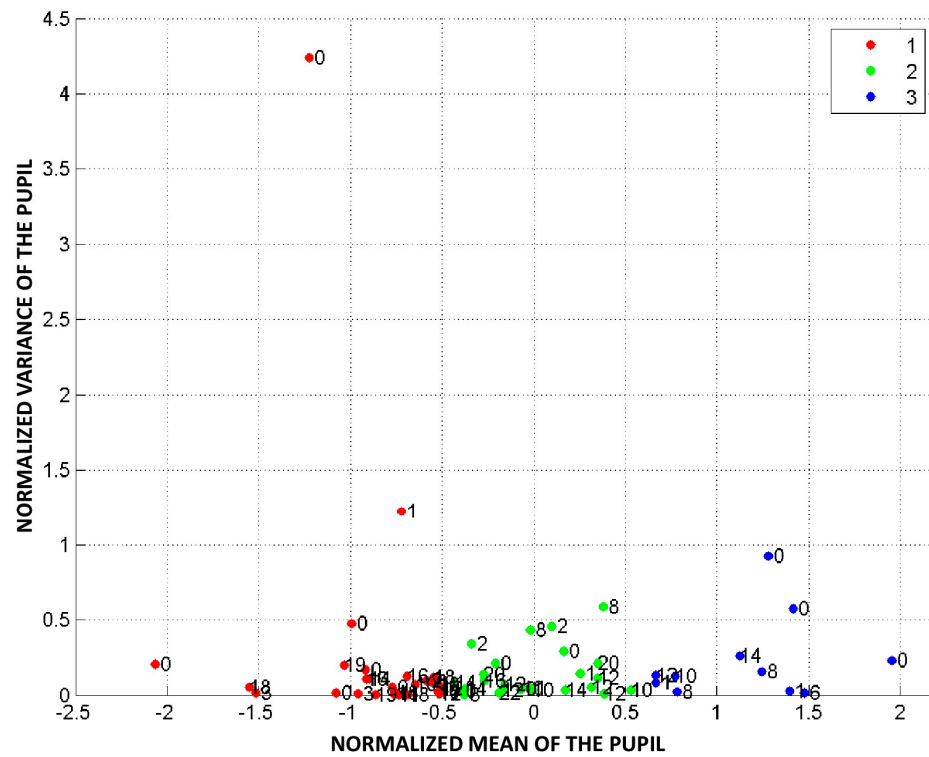
564 On average, the coefficients are over 0.75, so clustering is accepted as valid. For example, for the  
565 clusters in Figure 5, the Jaccard indices are 0.6288 (cluster 1), 0.9024 (cluster 2), and 0.8517 (cluster 3).  
566 Considering all the valid participants, the number of clusters varies between three and six levels of  
567 mental workload, and on average, there are approximately four levels of mental workload validated  
568 with acceptable cohesion indices (RQ1).

569

570



571  
 572 **Figure 4.** Optimal number of clusters according to the intersection method of CH and WSS curves  
 573 for participant 59.  
 574  
 575



576  
 577 **Figure 5.** Optimal grouping of time windows according to their level of cognitive load for the  
 578 participant 59.

#### 579 4.4.5 Machine Learning Models and Feature Selection

580 To perform the classification, a training set is first generated with 70 % of the observations and  
 581 then a test set with the remaining 30 %. To avoid biases, a 10-fold cross validation is performed in  
 582 which the classes are distributed uniformly within each set. In addition, they are randomly selected  
 583 while maintaining the proportions. Because clustering generates some classes containing very few

584 elements, sometimes just one or two, time windows that would not make sense to classify because  
 585 they would only be in the training set and not in the test set, are deleted.

586 Two classification models are applied: artificial neural networks and recursive feature  
 587 elimination (NN and RFE respectively) and two-layer multi-layer perceptron (MLP). Each  
 588 classification result is obtained from the average resulting from executing each algorithm 100 times.  
 589 Next, the implementation of each model is described.

590 An artificial neural network with a hidden layer is implemented, with all the artificial neurons  
 591 completely interconnected and trained with the algorithm backpropagation. To calculate the  
 592 number of neurons in the hidden layer ( $h$ ), the heuristic method of the geometric pyramid rule is  
 593 used with the expression  $h = \sqrt{m \cdot n}$ , which consists in calculating the square root of the product  
 594 between the number of inputs ( $m$ ) – number of characteristics – and the number of outputs ( $n$ ) –  
 595 number of classes. Therefore, the number of neurons in the hidden layer changes per participant.  
 596 This classifier is combined with the RFE method for feature selection.

597 There is evidence in the literature regarding the use of the random forest and recursive feature  
 598 elimination (RF-RFE) method for the selection of characteristics with good results when applied to  
 599 the classification of mental fatigue with EEG signals [99]. This combines recursive elimination with  
 600 random forest, that is, a set of decision trees that assesses features and generates a ranking following  
 601 a score criterion. This method of feature selection is implemented with the Caret and Random Forest  
 602 packages in R. The algorithm is executed using Matlab's Neural Network Toolbox with the toolbox's  
 603 Neural Net Pattern Recognition nprtool. It is executed once the characteristics have been obtained –  
 604 per participant – with the RFE method. Table 3 shows the characteristics selected for six participants  
 605 as an example.

606 To test another way of improving the artificial neural network without using feature selection, a  
 607 different neural network configuration is tested: MLP. For the implementation of the MLP neural  
 608 network, the H2O package in R is used [100]. The programmed neural network has two hidden  
 609 layers with 100 neurons each, with a rectified linear activation function, as used by Hinton [101]. The  
 610 key, according to Hinton, to reducing overfitting is to include a 50 % dropout for each layer, which  
 611 prevents artificial neurons from co-adapting to training data.

612

613 **Table 3.** Selected features with the RFE method for different participants.

614

Participant	Selected features
1	maxPhasic, meanECGMAD, meanHR, powerEEG channel1, phaseEEG channel1, powerEEG channel3, phaseEEG channel12
2	medianTemp, avgGSR, powerEEG channel7, phaseEEG channel7, powerEEG channel1, powerEEG channel11
3	meanHR, meanPhasic, phaseEEG channel8, meanECGMAD, maxPhasic, rmsHR, accGSR, powerEEG channel5, phaseEEG channel4, phaseEEG channel6, phaseEEG channel12, avgGSR, stdHR, phaseEEG channel2, phaseEEG channel7, meanTemp, phaseEEG channel5, phaseEEG channel13, powerEEG channel13, phaseEEG channel1, medianECGMAD, powerEEG channel2, phaseEEG channel14, varECGMAD
4	meanHR, avgGSR, powerEEG channel1, phaseEEG channel9, powerEEG channel13, phaseEEG channel14, medianTemp, varECGMAD, phaseEEG channel2, rmsHR, mean-Phasic, phaseEEG channel8, medianECGMAD, phaseEEG channel1, phaseEEG channel12, numpksPhasic, phaseEEG channel11, phaseEEG channel13, maxPhasic, powerEEG channel8
5	avgGSR, meanTemp
6	medianTemp, powerEEG channel6, powerEEG channel5, meanPhasic

615 Thus, each neuron in the hidden layers is omitted at random from the network with a  
 616 probability of 0.5. In addition, another method added to avoid model overfitting is the  $L_1$  and  $L_2$   
 617 regularization method as a linear combination, as shown in Equation (7)**Error! Reference source not**  
 618 **found.** For this, the objective function for the artificial neural network is defined as  $L(\mathbf{W}, \mathbf{B}|j)$ ,  
 619 where  $\mathbf{W}$  represents the weight matrix and  $\mathbf{B}$  the column of bias vectors for each training example.  
 620

$$L'(\mathbf{W}, \mathbf{B}|j) = L(\mathbf{W}, \mathbf{B}|j) + \lambda_1 R_1(\mathbf{W}, \mathbf{B}|j) + \lambda_2 R_2(\mathbf{W}, \mathbf{B}|j) \quad (7),$$

621  
 622 where the values of  $\lambda_1$  and  $\lambda_2$  are parameters that weight the relative contribution of the penalty  
 623 terms  $R_1$  and  $R_2$  (rule  $L_1$  and  $L_2$ , respectively) in relation to the objective function  $L(\mathbf{W}, \mathbf{B}|j)$ . The  
 624 values of  $\lambda_1 = 10^{-5}$  and  $\lambda_2 = 10^{-5}$  are determined as recommended in the H20 manual [100].

## 625 5. Results

### 626 5.1 Statistical Analysis

627 Based on Bailey (2008) [23], who showed a decrease in mental workload between subtask  
 628 boundaries, the hypothesis that there is a decrease in mental workload in the transition time  
 629 windows between the analysis time windows of one Web element and another is proposed. To  
 630 verify the hypothesis, the mean pupil diameter within each window is selected as our gold standard.  
 631 The objective is to determine if mean pupil diameter varies depending on whether it is in an active  
 632 window or in a transition object. An analysis of variance with repeated measures (ANOVA-RM) is  
 633 performed since the factors to be studied are within-subjects. For the analysis, the complete universe  
 634 of windows of all the participants is considered.

635 As a result, a  $p - value = 0.00184$  is obtained with a 95 % confidence interval, so the null  
 636 hypothesis is rejected. In addition, as shown in Table 4, mean pupil diameter in the transition  
 637 windows is smaller than in the active windows. Therefore, it is concluded for the data as a whole  
 638 that the difference between mean pupil diameter in the active windows and the transition windows  
 639 is statistically significant and that the diameter is smaller in the transition windows (H1).

### 640 5.2 Classification

641 Table 5 shows that the worst accuracy measure obtained with the NN-RFE is 45.24 %  
 642 (participant 48) with five classes, and the best result is 95.24 % (participant 23) with two classes. The  
 643 classification mean including all 53 participants yields the result of 68.94 % accuracy with a standard  
 644 deviation of 11.54 %. The results of the classification according to the number of final classes are also  
 645 analyzed. As shown in Table 6, there is a tendency for the classification percentage to decrease as the  
 646 number of classes increases. In particular, an accuracy of 90.61 % is obtained for the classification of  
 647 two classes, 73.34 % for three classes and acceptable values are obtained for four and five classes.

648 Regarding the MLP, in Table 7, the worst measure of accuracy obtained is 72.16 % (participant  
 649 17) with four classes, and the best result is 99.9 % (participant 9) with three classes. The classification  
 650 mean including all 53 participants is 88.46 % with a standard deviation of 7.94 % for the accuracy  
 651 measure (RQ2). The classification analysis is performed according to the number of final classes. As  
 652 shown in Table 8, the trend observed for NN-RFE is maintained such that the higher the number of  
 653 classes is, the lower the classification percentage, but with a break in the case of four and five classes.

656 **Table 4.** Standardized means of pupillary diameter for transition and active windows.  
 657

Factor	Mean	Standard Deviation
Transition	0.01924	0.97
Active	0.10737	0.84

659  
660**Table 5.** Results of classification using NN-RFE.

-	Accuracy (%)	Recall (%)	Precision (%)
Mean	68.94	66.62	76.92
Standard Deviation	11.54	13	11.62
Maximum	95.24	95.45	95.45
Minimum	45.24	39.99	46.29

661  
662  
663  
664**Table 6.** Average classification using NN-RFE by quantity of classes.

Number of classes	Accuracy (%)	Recall (%)	Precision (%)
2	90.61	89.99	92.15
3	73.34	71.69	83.56
4	63.29	59.57	70.75
5	57.94	54.92	64.35
6	53.85	53.61	66.31

665  
666  
667  
668**Table 7.** Results of classification using MLP.

-	Accuracy (%)	Recall (%)	Precision (%)
Mean	99.1	98.99	99.27
Standard Deviation	0.2722	0.3325	0.2174
Maximum	100	100	100
Minimum	98.26	97.96	98.64

669  
670  
671**Table 8.** Average classification using MLP by quantity of classes.

Number of classes	Accuracy (%)	Recall (%)	Precision (%)
2	99.03	98.92	99.22
3	99.14	99.05	99.31
4	99.06	98.93	99.25
5	99.06	98.96	99.24
6	99.22	99.15	99.36

672

673 *5.3 Evaluating Psychophysiological Sensors*

674 To assess the performance of each sensor, the MLP neural network that obtains the best results  
 675 with all the sensors is selected as a supervised learning model. Table 9 shows the results of assessing  
 676 the performance of each sensor separately. The sensor with the best performance is EEG, with 88.78  
 677 % accuracy in the classification, slightly superior to the classification using all the sensors. The other  
 678 sensors separately have a very low level of classification accuracy.  
 679

680 **Table 9.** Summary of sensor classification results for MLP with 100 neurons in each hidden layer and  
 681 400 epochs.  
 682

Sensors	Accuracy (%)	Recall (%)	Precision (%)
All	99.1	98.99	99.27
EDA	53.28	63.18	53.52
ST	42.37	76.41	35.7
ECG	46.22	66.81	45.55
PPG	46.69	76.58	43.88
EEG	92.27	94.74	94.94
EDA+PPG	63.36	68.33	66.5
EDA+EEG	96.23	97.44	97.73
PPG+EEG	95.89	96.78	96.56
EDA+PPG+EEG	97.29	98.01	98.36

683  
 684 Then, combinations of the three sensors with higher performance are tested: EEG, EDA, and  
 685 PPG (HR). As shown in Table 9, the combinations with EEG provide the best results. The  
 686 combination with the highest performance is EDA, PPG (HR), and EEG, with 95.73 %.

687 An important difference between the EEG sensor and the others is that it allows the extraction  
 688 of a greater number of characteristics because the 14 electrodes contribute two characteristics each,  
 689 for a total of 28 characteristics. This factor may explain the superior performance of this sensor  
 690 compared to the rest. Therefore, it is concluded that it is possible to obtain good classification results  
 691 for this experimental design with less than 5 sensors, even only with the EEG. The temperature  
 692 sensor and the ECG can thus be discarded.

#### 693 5.4 Evaluating Time Overhead

694 For mental workload classification in Web site browsing to lead to a real application, processing  
 695 must be sufficiently fast, given that the time windows considered have a minimum length of 500  
 696 milliseconds. Table 10 shows the classification time for the algorithms used that yielded the best  
 697 results.

698 The results show that, for the artificial neural networks and RFE model, the time window is  
 699 very small at 0.0083 seconds on average, which ensures that this model can be implemented in real  
 700 time with an acceptable classification mean of 68.94 % (see Table 5).

701

702 **Table 10.** Testing time for models.  
 703

	Mean [sec]	Standard Deviation [sec]
NN-RFE	0.0083	0.001
MLP	0.109	0.023
MLP EEG	0.1218	0.0041
MLP EDA+PPG	0.1056	0.0091
MLP EDA+EEG	0.1207	0.0098
MLP PPG+EEG	0.107	0.0037
MLP EDA+PPG+EEG	0.126	0.007

704  
 705

706 On the other hand, for the model based on MLP, the effect of its parameters given by the 100  
707 neurons in the two hidden layers increases the processing time to an average of 0,1 seconds. So, this  
708 model can be implemented in real time as well with a classification average of 99.1 % accuracy for all  
709 sensors and a reasonable 63.36% for more portable sensors (PPG and EDA, see Table 9).

## 710 6. Discussion

711 The results of the statistical analysis determine that pupil diameter in the transition time  
712 windows is statistically and significantly lower than in the active windows of Web element analysis.  
713 Given the proven correlation between pupil dilation and mental workload, it is determined that  
714 there is a decrease in mental workload in the time windows between the analysis of one Web  
715 element and another (H1).

716 A possible application of the demonstration of this hypothesis (H1) is the generation of  
717 recommendation systems that support the user in during Web browsing according to her interest,  
718 that is, when she is not cognitively overloaded with new content. This is applicable, for example, to  
719 retail applications or advertisement.

720 Regarding the assessment of the psychophysiological sensors to estimate mental workload,  
721 with the exception of the EEG, the signals of the sensors used do not provide an appropriate level of  
722 classification by themselves for this type of task, although the combinations of signals with EEG  
723 stand out, obtaining very good results. One of the reasons may be the time constant of each signal;  
724 that is, signals such as skin temperature or conductivity take longer to react compared to electrical  
725 signals from the brain.

726 However, despite the fact that the combination of EDA and PPG (HR) does not provide better  
727 results than EEG alone, a reasonable level of accuracy (63.36 %) is obtained for its use in practice,  
728 even before portable EEG technology is available. The advantage of the EDA and PPG sensors is that  
729 they are non-invasive, portable, cheaper, and easily integrated into a board that transmits via  
730 Bluetooth or other wireless means to a gateway, such as a smartphone, from a wearable such as a  
731 smartwatch, a wristband, or a textile [88]. In addition, considering that the time overhead of the  
732 classification in each time window is very small (on average 0.1056 s, with a standard deviation of  
733 0.0091 s), EDA and PPG are considered feasible alternatives for the first practical applications of the  
734 real-time assessment of mental workload in users browsing Web pages.

## 735 7. Conclusion

736 The study of human behavior and physiology when performing human-computer interactions  
737 activities is complex due to the multiple factors that affect each person in their performance and  
738 behavior with regard to this class of tasks. This research assesses the behavior of a user in the simple  
739 task of browsing freely through a fictitious Web page created specifically for this study, using  
740 psychophysiological sensors.

741 It is shown that for the complete data set, that is, considering the complete universe of windows  
742 of all the participants, pupil diameter – as a measure of mental workload – is significantly lower in  
743 the transition windows than in the active windows, with a significance of  $p - value = 0.00184$  for a  
744 95 % confidence interval. Therefore, patterns of low mental workload states are identified, and the  
745 hypothesis (H1) that it is indeed possible to measure mental workload in Web browsing activities  
746 and, moreover, that the mental workload of the user decreases in the transition from the analysis of  
747 one Web element to another while browsing freely is verified.

748 The unsupervised model of k-means analysis as a data mining technique is applied to the mean  
749 and variance of pupil dilation, based on which the Web browsing task involves on average four  
750 levels of mental workload. Thus, it is concluded that there are several mental workload states that  
751 can be determined (RQ1).

752 To classify levels of mental workload, the MLP neural network is used, which obtains a result of  
753 88.46 % accuracy on average (RQ2). In addition, the electroencephalogram is the sensor that obtains  
754 the best results, classifying with 88.78 % accuracy. If the EEG is combined with the PPG and EDA,  
755 the accuracy of the classification rises to 95.73 %.

756 In terms of future lines of research, it is proposed to use the data to study Web users' mood  
757 behavior together with their cognitive behavior. In addition, it is proposed to focus the research on  
758 the EEG sensor, which showed superior performance, using other analytical approaches, such as  
759 wavelets and/or ERP, to determine the most relevant involved brain areas.

760 **Supplementary Materials:** The following dataset was submitted as supplementary material: "dataset\_Sensors".  
761 It contains all the preprocessed, gathered sensor data for each participant.

762 **Acknowledgments:** This work was financed by the CONICYT FONDECYT program, project code: 11130252.  
763 The authors are thankful for the continuous support of "Instituto Sistemas Complejos de Ingeniería"  
764 (CONICYT: Proyecto Basal FBO16). In addition, the authors would like to thank Todd Pezzuti, Marcos Orchard,  
765 Javier Ruiz-del-Solar and all the experiment participants.

766 **Author Contributions:** Angel Jimenez-Molina initiated the research, conceived and designed the experiments;  
767 Cristian Retamal performed the experiments; Cristian Retamal and Herman Lira analyzed the data; Angel  
768 Jimenez-Molina and Cristian Retamal wrote the paper.

769 **Conflicts of Interest:** The authors declare no conflict of interest.

## 770 References

- 771 1. Landauer, T. *The trouble with computers: Usefulness, usability, and productivity*; MIT Press, 1995; Vol. 11;  
772 ISBN 0262121867.
- 773 2. Gwizdka, J. Distribution of cognitive load in Web search. *J. Am. Soc. Inf. Sci. Technol.* **2010**, *61*, 2167–  
774 2187, doi:10.1002/asi.21385.
- 775 3. Albers, M. J. Tapping as a measure of cognitive load and website usability. *Proc. 29th ACM Int. Conf.*  
776 *Des. Commun. - SIGDOC '11* **2011**, *25*, doi:10.1145/2038476.2038481.
- 777 4. Longo, L.; Rusconi, F.; Noce, L.; Barrett, S. The importance of Human Mental Workload in Web  
778 Design. *Proc. 8th Int. Conf. Web Inf. Syst. Technol.* **2012**, 403–409, doi:10.5220/0003960204030409.
- 779 5. Buscher, G.; Cutrell, E.; Morris, M. R.; Buscher, G., Cutrell, E. and Morris, M. R. 2009. What do you see  
780 when you're surfing?: Using eye tracking to predict salient regions of web pages. In *Proceedings of the*  
781 *27th international conference on Human factors in computing systems - CHI 09*; In *Proceedings CHI 2009*,  
782 21-30.: New York, New York, USA, 2009; p. 21.
- 783 6. Buscher, G.; Dumais, S. T.; Cutrell, E.; Buscher, G., Dumais, S. and Cutrell, E. 2010. The good, the bad,  
784 and the random: an eye-tracking study of ad quality in web search. In *Proceeding of the 33rd*  
785 *international ACM SIGIR conference on Research and development in information retrieval - SIGIR '10*; In  
786 *Proceedings SIGIR 2010*.: New York, New York, USA, 2010; p. 42.
- 787 7. Dumais, S. T.; Buscher, G.; Cutrell, E. Individual differences in gaze patterns for web search. In  
788 *Proceeding of the third symposium on Information interaction in context - IIiX '10*; ACM Press: New York,  
789 New York, USA, 2010; p. 185.
- 790 8. Sweller, J. Cognitive Load During Problem Solving: Effects on Learning. *Cogn. Sci.* **1988**, *12*, 257–285,  
791 doi:10.1207/s15516709cog1202\_4.
- 792 9. Wickens, C. D. Multiple resources and performance prediction. *Theor. Issues Ergon. Sci.* **2002**, *3*, 159–  
793 177, doi:10.1080/1463922010123806.
- 794 10. Parasuraman, R.; Sheridan, T. B.; Wickens, C. D. Situation Awareness, Mental Workload, and Trust in  
795 Automation: Viable, Empirically Supported Cognitive Engineering Constructs. *J. Cogn. Eng. Decis. Mak.*  
796 **2008**, *2*, 140–160, doi:10.1518/155534308X284417.
- 797 11. Arbib, M. A.; Bonaiuto, J. J. *From neuron to cognition via computational neuroscience*; ISBN 9780262034968.
- 798 12. Jung J., Maier A., Gross A., Ruiz N., Chen F., Yin B. 2011. *Investigating the Effect of Cognitive Load on*  
799 *UX: A Driving Study.*; AutomotiveUI'11, November 29-December 2, 2011, Salzburg, Austria Adjunct

800 Proceedings.

801 13. Paas, F.; Tuovinen, J. E.; Tabbers, H.; Van Gerven, P. W. M. Cognitive Load Measurement as a Means  
802 to Advance Cognitive Load Theory. *Educ. Psychol.* **2003**, *38*, 63–71, doi:10.1207/S15326985EP3801\_8.

803 14. Nguyen, Frank, Colvin-Clark, R. Learning Solutions, November 7, 2005. 2005.,

804 15. van Merriënboer, J. J. G.; Ayres, P. Research on cognitive load theory and its design implications for  
805 e-learning. *Educ. Technol. Res. Dev.* **2005**, *53*, 5–13, doi:10.1007/BF02504793.

806 16. Fritz, T.; Begel, A.; Müller, S. C.; Yigit-Elliott, S.; Züger, M. Using psycho-physiological measures to  
807 assess task difficulty in software development. In *Proceedings of the 36th International Conference on*  
808 *Software Engineering - ICSE 2014*; International Conference on Software Engineering (ICSE),  
809 Hyderabad, pp 402-413.: New York, New York, USA, 2014; pp. 402–413.

810 17. Haapalainen, E.; Kim, S.; Forlizzi, J. F.; Dey, A. K. Psycho-physiological measures for assessing  
811 cognitive load. In *Proceedings of the 12th ACM international conference on Ubiquitous computing - Ubicomp*  
812 '10; Proceedings of the 12th ACM International Conference on Ubiquitous Computing, pp. 301–310.,  
813 2010.

814 18. Ikehara, C. S.; Crosby, M. E. Assessing Cognitive Load with Physiological Sensors. In *Proceedings of the*  
815 *38th Annual Hawaii International Conference on System Sciences*; IEEE; p. 295a–295a.

816 19. Hogervorst, M. A.; Brouwer, A.-M.; van Erp, J. B. F. Combining and comparing EEG, peripheral  
817 physiology and eye-related measures for the assessment of mental workload. *Front. Neurosci.* **2014**, *8*,  
818 322, doi:10.3389/fnins.2014.00322.

819 20. Khusainov, R.; Azzi, D.; Achumba, I. E.; Bersch, S. D. Real-time human ambulation, activity, and  
820 physiological monitoring: Taxonomy of issues, techniques, applications, challenges and limitations.  
821 *Sensors (Switzerland)* **2013**, *13*, 12852–12902.

822 21. Gazzaniga, M. S.; Ivry, R. B.; Mangun, G. R. Cognitive Neuroscience: The Biology of the Mind. *Q. Rev.*  
823 *Biol.* **2009**, *84*, 196–197.

824 22. Davis, Stephen, Palladino, J.; Stephen F. Davis, Joseph J. Palladino, Christopherson, K. *Psychology*;  
825 Pearson, 2012; ISBN 0205848559.

826 23. Bailey, B. P.; Iqbal, S. T. Understanding changes in mental workload during execution of goal-directed  
827 tasks and its application for interruption management. *ACM Trans. Comput. Interact.* **2008**, *14*, 1–28,  
828 doi:10.1145/1314683.1314689.

829 24. Hess, E. H.; Polt, J. M. Pupil Size in Relation to Mental Activity during Simple Problem-Solving. *Science*  
830 (80-. ). **1964**, *143*, 1190–1192, doi:10.1126/science.143.3611.1190.

831 25. Hahnemann, D.; Beatty, J.; Kahneman, D.; Beatty, J. Pupillary responses In a pitch-discrimination task.  
832 *Percept. Psychophys.* **1967**, *2*, 101–105, doi:10.3758/BF03210302.

833 26. Juris, M.; Velden, M. The pupillary response to mental overload. *Physiol. Psychol.* **1977**, *5*, 421–424,  
834 doi:10.3758/BF03337847.

835 27. Beatty, J. Task-evoked pupillary responses, processing load, and the structure of processing resources.  
836 *Psychol. Bull.* **1982**, *91*, 276–92.

837 28. Hoeks, B.; Levelt, W. J. M. Pupillary dilation as a measure of attention: a quantitative system analysis.  
838 *Behav. Res. Methods, Instruments, Comput.* **1993**, *25*, 16–26, doi:10.3758/BF03204445.

839 29. Nakayama, M.; Takahashi, K.; Shimizu, Y. The act of task difficulty and eye-movement frequency for  
840 the “Oculo-motor indices.” In *Proceedings of the symposium on Eye tracking research & applications* -  
841 *ETRA '02*; Proceedings of Eye Tracking Research and Applications.: New York, New York, USA, 2002;  
842 p. 37.

843 30. Li, G.; Lee, B. L.; Chung, W. Y. Smartwatch-Based Wearable EEG System for Driver Drowsiness  
844 Detection. *IEEE Sens. J.* **2015**, *15*, 7169–7180, doi:10.1109/JSEN.2015.2473679.

845 31. Brockmeier, A. J.; Príncipe, J. C. Learning recurrent waveforms within EEGs. *IEEE Trans. Biomed. Eng.*  
846 **2016**, *63*, 43–54, doi:10.1109/TBME.2015.2499241.

847 32. SmartCap Technologies Available online: <https://www.smartcaptech.com/> (accessed on Dec 2, 2017).

848 33. Oulasvirta, A.; Tamminen, S.; Roto, V.; Kuorelahti, J. Interaction in 4-Second Bursts: The Fragmented  
849 Nature of Attentional Resources in Mobile HCI. *Proc. SIGCHI Conf. Hum. factors Comput. Syst. - CHI '05*  
850 **2005**, 919, doi:10.1145/1054972.1055101.

851 34. Fawcett, J. M.; Risko, E. F.; Kingstone, A. *The handbook of attention*; 2015; ISBN 9780262029698.

852 35. Navon, D.; Gopher, D. On the economy of the human-processing system. *Psychol. Rev.* **1979**, *86*, 214–  
853 255, doi:10.1037/0033-295X.86.3.214.

854 36. Matthews, G.; Warm, J. S.; Smith, A. P. Task Engagement and Attentional Resources. *Hum. Factors J.*  
855 *Hum. Factors Ergon. Soc.* **2017**, *59*, 44–61, doi:10.1177/0018720816673782.

856 37. Miettinen, M.; Oulasvirta, A. Predicting time-sharing in mobile interaction. *User Model. User-adapt.*  
857 *Interact.* **2007**, *17*, 475–510, doi:10.1007/s11257-007-9033-x.

858 38. Jimenez-Molina, A.; Ko, I.-Y. Cognitive resource-aware unobtrusive service provisioning in ambient  
859 intelligence environments. *J. Ambient Intell. Smart Environ.* **2015**, *7*, doi:10.3233/AIS-140299.

860 39. Norman, D. A.; Draper, S. W. *USER CENTERED SYSTEM DESIGN New Perspectives on*  
861 *Human-Computer Interaction Library of Congress Cataloging-in-Publication Data*; 1986; ISBN 0-89859-872-9.

862 40. Monk, C. A.; Boehm-Davis, D. A.; Trafton, J. G. The Attentional Costs of Interrupting Task  
863 Performance at Various Stages. *Proc. Hum. Factors Ergon. Soc. Annu. Meet.* **2002**, *46*, 1824–1828,  
864 doi:10.1177/154193120204602210.

865 41. Young, M. S.; Brookhuis, K. A.; Wickens, C. D.; Hancock, P. A. State of science: mental workload in  
866 ergonomics. *Ergonomics* **2015**, *58*, 1–17, doi:10.1080/00140139.2014.956151.

867 42. Matthews, G.; Reinerman-Jones, L. E.; Barber, D. J.; Abich, J. The Psychometrics of Mental Workload:  
868 Multiple Measures Are Sensitive but Divergent. *Hum. Factors J. Hum. Factors Ergon. Soc.* **2015**, *57*, 125–  
869 143, doi:10.1177/0018720814539505.

870 43. Greco, A.; Valenza, G.; Scilingo, E. P. Emotions and Mood States: Modeling, Elicitation, and  
871 Recognition. In *Advances in Electrodermal Activity Processing with Applications for Mental Health*; Springer  
872 International Publishing: Cham, 2016; pp. 45–54.

873 44. Guastello, S. J.; Shircel, A.; Malon, M.; Timm, P. Individual differences in the experience of cognitive  
874 workload. *Theor. Issues Ergon. Sci.* **2015**, *16*, 20–52, doi:10.1080/1463922X.2013.869371.

875 45. Dhami, M. K.; Hertwig, R.; Hoffrage, U. The Role of Representative Design in an Ecological Approach  
876 to Cognition. *Psychol. Bull.* **2004**, *130*, 959–988, doi:10.1037/0033-2909.130.6.959.

877 46. Hart, S. G.; Staveland, L. E. Development of NASA-TLX (Task Load Index): Results of Empirical and  
878 Theoretical Research. *Adv. Psychol.* **1988**, *52*, 139–183, doi:10.1016/S0166-4115(08)62386-9.

879 47. Halverson, T.; Estepp, J.; Christensen, J.; Monnin, J. Classifying Workload with Eye Movements in a  
880 Complex Task. *Proc. Hum. Factors Ergon. Soc. Annu. Meet.* **2012**, *56*, 168–172,  
881 doi:10.1177/1071181312561012.

882 48. Mehler, B.; Reimer, B.; Coughlin, J. F. Sensitivity of Physiological Measures for Detecting Systematic  
883 Variations in Cognitive Demand From a Working Memory Task. *Hum. Factors* **2012**, *54*, 396–412,  
884 doi:10.1177/0018720812442086.

885 49. Wang, S.; Gwizdka, J.; Chaovallitwongse, W. A. Using Wireless EEG Signals to Assess Memory

886 Workload in the n-Back Task. *IEEE Trans. Human-Machine Syst.* **2016**, *46*, 424–435,  
887 doi:10.1109/THMS.2015.2476818.

888 50. Cacioppo, Tassinary, Berntson. 2007. *The Handbook of Psychophysiology.*; Cacioppo, J. T., Tassinary, L. G.,  
889 Berntson, G. G., Eds.; Cambridge University Press. Third Edition: Cambridge, 2017; ISBN  
890 9781107415782.

891 51. Walsh, E. G.; Marshall, J. *Physiology of the nervous system*; Longmans London, 1957;

892 52. Mohino-Herranz, I.; Gil-Pita, R.; Ferreira, J.; Rosa-Zurera, M.; Seoane, F. Assessment of Mental,  
893 Emotional and Physical Stress through Analysis of Physiological Signals Using Smartphones. *Sensors*  
894 **2015**, *15*, 25607–25627, doi:10.3390/s151025607.

895 53. Nardelli, M.; Valenza, G.; Cristea, I. A.; Gentili, C.; Cotet, C.; David, D.; Lanata, A.; Scilingo, E. P.  
896 Characterizing psychological dimensions in non-pathological subjects through autonomic nervous  
897 system dynamics. *Front. Comput. Neurosci.* **2015**, *9*, 37, doi:10.3389/fncom.2015.00037.

898 54. Banaee, H.; Ahmed, M. U.; Loutfi, A. Data mining for wearable sensors in health monitoring systems: a  
899 review of recent trends and challenges. *Sensors* **2013**, *13*, 17472–17500, doi:10.3390/s131217472.

900 55. Goldberg, J. H.; Wichansky, A. M. Eye Tracking in Usability Evaluation. In *The Mind's Eye*; In Hyona,  
901 J., Radach, R., & Deubel, H. (Eds.), The mind's eye: Cognitive and applied aspects of eye movement  
902 research (pp. 493–516). Amsterdam:Elsevier., 2003; pp. 493–516 ISBN 9780444510204.

903 56. Kuipers, J.-R.; Thierry, G. ERP-pupil size correlations reveal how bilingualism enhances cognitive  
904 flexibility. *Cortex* **2013**, *49*, 2853–2860.

905 57. Steinhauer, S. R.; Siegle, G. J.; Condray, R.; Pless, M. Sympathetic and parasympathetic innervation of  
906 pupillary dilation during sustained processing. *Int. J. Psychophysiol.* **2004**, *52*, 77–86.

907 58. Beatty, J.; Lucero-Wagoner, B. *The Pupillary System*; Handbook of psychophysiology, 2nd ed., (pp.  
908 142–162). New York, NY, US: Cambridge University Press., 2000;

909 59. Zhou, J.; Sun, J.; Chen, F.; Wang, Y.; Taib, R. Measurable Decision Making with GSR and Pupillary  
910 Analysis for Intelligent User Interface. *ACM Trans. Comput. Interact. - Spec. Issue Physiol. Comput.*  
911 *Human-Computer Interact.* **2015**, *21*, 1–23, doi:10.1145/2687924.

912 60. Andreassi, J. L. *sychophysiology: Human Behaviour and Physiological response*; 2000; ISBN 080582832X.

913 61. Brioschi, M. L.; Siqueira, J. T. T. de; Teixeira, M. J. Avanços da imagem infravermelha na disfunção  
914 temporomandibular. *JBA j. bras. oclus. ATM dor orofac* **2006**, *6*, 34–41.

915 62. Genno, H.; Ishikawa, K.; Kanbara, O.; Kikumoto, M.; Fujiwara, Y.; Suzuki, R.; Osumi, M. Using facial  
916 skin temperature to objectively evaluate sensations. *Int. J. Ind. Ergon.* **1997**, *19*, 161–171,  
917 doi:10.1016/S0169-8141(96)00011-X.

918 63. Angeles-Aquino, F.; Cantu-Chapa, A. Subsurface Upper Jurassic stratigraphy in the Campeche Shelf,  
919 Gulf of Mexico. *West. Gulf Mex. Basin. Tectonics, Sediment. Basins, Pet. Syst.* **2001**, *75*, 343–352,  
920 doi:fzbgvk.

921 64. Latorella, K. A. Effects of Modality on Interrupted Flight Deck Performance: Implications for Data  
922 Link. *Proc. Hum. Factors Ergon. Soc. Annu. Meet.* **1998**, *42*, 87–91, doi:10.1177/154193129804200120.

923 65. Speier, C.; Valacich, J. S.; Vessey, I. The Influence of Task Interruption on Individual Decision Making:  
924 An Information Overload Perspective. *Decis. Sci.* **1999**, *30*, 337–360,  
925 doi:10.1111/j.1540-5915.1999.tb01613.x.

926 66. Zijlstra, F. R. H.; Roe, R. A.; Leonora, A. B.; Krediet, I. Temporal factors in mental work: Effects of  
927 interrupted activities. *J. Occup. Organ. Psychol.* **1999**, *72*, 163–185, doi:10.1348/096317999166581.

928 67. Adamczyk, P. D.; Bailey, B. P. If not now when?: the effects of interruption at different moments

929 within task execution. *Proc. SIGCHI Conf. Hum. factors Comput. Syst.* **2004**, *6*, 271–278,  
930 doi:10.1145/985692.985727.

931 68. Bailey, B. P.; Konstan, J. A. On the need for attention-aware systems: Measuring effects of interruption  
932 on task performance, error rate, and affective state. In *Computers in Human Behavior*; Pergamon, 2006;  
933 Vol. 22, pp. 685–708.

934 69. Miyata, Y.; Norman, D. Psychological issues in support of multiple activities. *User centered Syst. Des.*  
935 **1986**, 265–284.

936 70. Yoshida, Y.; Ohwada, H.; Mizoguchi, F.; Iwasaki, H. Classifying Cognitive Load and Driving Situation  
937 with Machine Learning. *Int. J. Mach. Learn. Comput.* **2014**, *4*, 210–215, doi:10.7763/IJMLC.2014.V4.414.

938 71. Shi et al. 2007. *Galvanic Skin Response (GSR) as an Index of Cognitive Load.*; CHI Extended Abstracts on  
939 Human Factors in Computing Systems.;

940 72. Nourbakhsh, N.; Wang, Y.; Chen, F.; Calvo, R. A. Using galvanic skin response for cognitive load  
941 measurement in arithmetic and reading tasks. In *Proceedings of the 24th Australian Computer-Human  
942 Interaction Conference on - OzCHI '12*; Conference: Proceedings of the 24th Australian  
943 Computer-Human Interaction Conference.: New York, New York, USA, 2012; pp. 420–423.

944 73. Xu, J.; Wang, Y.; Chen, F.; Choi, E. Pupillary Response Based Cognitive Workload Measurement under  
945 Luminance Changes. In; *Interact 2011*, Part II. LNCS, vol. 6947:178-185. Springer, Heidelberg., 2011; pp.  
946 178–185.

947 74. Navalpakkam, V.; Churchill, E. Mouse Tracking: Measuring and Predicting Users' Experience of  
948 Web-based Content. In *Proceedings of the 2012 ACM annual conference on Human Factors in Computing  
949 Systems - CHI '12*; In Proceedings of the ACM SIGCHI conference on human factors in computing  
950 systems (pp. 2963-2972). ACM Press.: New York, New York, USA, 2012; p. 2963.

951 75. Wearable Sensor Technology Available online: <https://www.shimmersensing.com/> (accessed on Dec 2,  
952 2017).

953 76. BITalino - Biomedical Equipment Available online: <http://bitalino.com/en/> (accessed on Dec 2, 2017).

954 77. Emotiv Available online: <https://www.emotiv.com/> (accessed on Dec 2, 2017).

955 78. Eye tracking technology for research - Tobii Pro Available online: <https://www.tobiipro.com/> (accessed  
956 on Dec 2, 2017).

957 79. Villarejo, M. V.; Zapirain, B. G.; Zorrilla, A. M. A stress sensor based on galvanic skin response (GSR)  
958 controlled by ZigBee. *Sensors.* **2012**, *12*, 6075–6101, doi:10.3390/s120506075.

959 80. Ye, Y.; He, W.; Cheng, Y.; Huang, W.; Zhang, Z. A Robust Random Forest-Based Approach for Heart  
960 Rate Monitoring Using Photoplethysmography Signal Contaminated by Intense Motion Artifacts.  
961 *Sensors.* **2017**, *17*, 385, doi:10.3390/s17020385.

962 81. Nelson, C. V; Geselowitz, D. B. *The theoretical basis of electrocardiology*; Oxford University Press, 1976;  
963 Vol. 1; ISBN 019857374X.

964 82. Macfarlane, P. W.; Lawrie, T. D. V. *Comprehensive electrocardiology: theory and practice in health and  
965 disease*; Pergamon, 1989; Vol. 2;

966 83. OpenSignals | Data Visualization Software | Bitalino Available online: <http://bitalino.com/en/software/>  
967 (accessed on Dec 2, 2017).

968 84. Tobii Pro Studio eye tracking software, dedicated for UX Available online:  
969 <https://www.tobiipro.com/product-listing/tobii-pro-studio/> (accessed on Dec 2, 2017).

970 85. iMotions Biometric Research Platform. 2016. *Eye Tracking Pocket Guide.*;

971 86. Parsons, H. M. What Happened at Hawthorne?: New evidence suggests the Hawthorne effect resulted

972 from operant reinforcement contingencies. *Science* (80- ). **1974**, *183*, 922–932,  
973 doi:10.1126/science.183.4128.922.

974 87. Loyola, P.; Martínez, G.; Muñoz, K.; Velásquez, J. D.; Maldonado, P.; Couve, A. Combining eye  
975 tracking and pupillary dilation analysis to identify Website Key Objects. *Neurocomputing* **2015**, *168*,  
976 179–189, doi:10.1016/J.NEUCOM.2015.05.108.

977 88. iMotions Biometric Research Platform. 2016. *GSR Pocket Guide.*;  
978 89. Li, X.; Chen, X.; Yan, Y.; Wei, W.; Wang, Z. J. Classification of EEG signals using a multiple kernel  
979 learning support vector machine. *Sensors*. **2014**, *14*, 12784–12802, doi:10.3390/s140712784.

980 90. Fauvel, S.; Ward, R. K. An energy efficient compressed sensing framework for the compression of  
981 electroencephalogram signals. *Sensors*. **2014**, *14*, 1474–1496, doi:10.3390/s140101474.

982 91. Quintero-Rincón, A. Preprocesamiento de EEG con Filtros Hampel. *ARGENCON 2012 - IEEE Lat. Am.*  
983 *Trans.*

984 92. Guyon, I.; Elisseeff, A. An Introduction to Feature Extraction. In *Feature Extraction; Feature Extraction.*  
985 Foundations and Applications 207:1–25: Berlin, Heidelberg, 2006; pp. 1–25.

986 93. Betella, A.; Zucca, R.; Cetnarski, R.; Greco, A.; LanatÁ, A.; Mazzei, D.; Tognetti, A.; Arsiwalla, X. D.;  
987 Omedas, P.; De Rossi, D.; Verschure, P. F. M. J. Inference of human affective states from  
988 psychophysiological measurements extracted under ecologically valid conditions. *Front. Neurosci.* **2014**,  
989 *8*, 286, doi:10.3389/fnins.2014.00286.

990 94. iMotions Biometric Research Platform. 2016. *EEG Pocket Guide.*;  
991 95. Cohen, M. X. *Analyzing neutral time series data. Theory and Practice*; Massachusetts Institute of  
992 Technology., 2014;

993 96. Xu, R.; Wunsch, D. C. *Clustering*; IEEE Press, 2009, John Wiley & Sons, Inc., Hoboken, New Jersey,  
994 USA. (pp. 263–278), 2009; ISBN 0470276800.

995 97. Zumel, N.; Mount, J. (Computational scientist) *Practical data science with R*; Manning Publications Co.  
996 1st Edition.; ISBN 9781617291562.

997 98. Calinski, T.; Harabasz, J. A dendrite method for cluster analysis. *Commun. Stat. - Theory Methods* **1974**,  
998 *3*, 1–27, doi:10.1080/03610927408827101.

999 99. Kai-Quan Shen, K.-Q.; Chong-Jin Ong, C.-J.; Xiao-Ping Li, X.-P.; Zheng Hui, Z.; Wilder-Smith, E. P. V.  
1000 A Feature Selection Method for Multilevel Mental Fatigue EEG Classification. *IEEE Trans. Biomed. Eng.*  
1001 **2007**, *54*, 1231–1237, doi:10.1109/TBME.2007.890733.

1002 100. Candel, A.; Lanford, J.; LeDell, E.; Parmar, V.; Arora, A. *Deep Learning with H2O*; Published by H2O.ai,  
1003 Inc. Third Edition., 2015;

1004 101. Hinton, G. E.; Srivastava, N.; Krizhevsky, A.; Sutskever, I.; Salakhutdinov, R. R. Improving neural  
1005 networks by preventing co-adaptation of feature detectors. **2012**.

1006

1007